Conducting Nanopearl Chains Based on the Dmit Salt

Guanglei Cui,[†,‡] Wei Xu*,[†] Chaowei Guo,[†,‡] Xunwen Xiao,[†,‡] Hai Xu,[†,‡] Deqing Zhang*,[†] Lei Jiang,*,[†] and Daoben Zhu[†]

Laboratory of Organic Solids, Center for Molecular Sciences, Institute of Chemistry, Chinese Academy of Sciences, 100080 Beijing, P. R. China and Graduate School of Chinese Academy of Sciences, Beijing, P. R. China

Received: April 25, 2004; In Final Form: June 27, 2004

Nanowire arrays of crystalline $[(CH_3)_4N][Ni(dmit)_2]_2$ have been fabricated by a galvanostatic electrochemical deposition method using anodic aluminum oxide as the template. A nanopearl chain structure associated with the oscillation of the voltage during the electrochemical deposition process was investigated. These nanowire arrays are highly textured as determined by XRD. The preliminary results show that the conductivities of the nanowires are in the semiconductor range.

Introduction

Nanometer scale materials have received broad attention in recent years because of their novel properties and potential applications.[1] Owing to high electrical conductivity, high mechanical flexibility, and potential applications in nanodevices,[2] 1D nanostructures of conducting polymers have been extensively studied. However, studies on 1D nanostructures of crystalline organic conducting materials are still rare, and only a few successful examples have been reported.[3] Unlike conducting polymers, crystalline organic conducting materials have well-defined structures (usually they have been studied as single crystals), which is good for understanding the charge transport and phase transition.[4] Transition-metal complexes with bis(dithiolate) ligands, such as dmit (dmit = $C_3S_5^{2-}$ = 2-thioxo-1,3-dithiole-4,5-dithiolato), are widely studied for their semiconducting, conducting, and even superconducting properties.[5] Here, we describe crystalline $Ni(dmit)_2$ nanowire arrays prepared by an electrochemical deposition method using anodic aluminum oxide (AAO) film as template.

Experimental Section

1. $[(CH_3)_4N][Ni(dmit)_2]$ (for the structure formula see Scheme 1) was prepared according to the literature.[6] It was characterized by Element Analyzer (Carlo-Erba-1106 instrument). Anal. calcd for $C_{10}H_{12}NS_{10}Ni$: C, 22.85; H, 2.30; N, 2.66; S, 61.01. Found: C, 22.88; H, 2.36; N, 2.68; S, 61.23.

2. Cyclic voltammograms were conducted in acetonitrile solution of 0.001 M $[(CH_3)_4N]$ $[Ni(dmit)_2]$ containing 0.1 M Bu_4NPF_6 as electrolyte using an EG&G potentiostat/Galvanostat Model 283 instruments. A standard platinum disk electrode (ϕ = 2 mm) was employed as working electrode with platinum wire (ϕ = 1 mm) as counter electrode and the saturated calomel electrode (SCE) as reference electrode. This experiment was carried out under room temperature.

3. All galvanostatic measurements was carried out in an acetonitrile solution of 0.001 M $[(CH_3)_4N][Ni(dmit)_2]$ and 0.01 M $[(CH_3)_4N][ClO_4]$ using EG&G potentiostat/Galvanostat Model 283 instruments. The electrodeposition was performed under 25 °C according to literature.[2] Nanowire arrays were produced by electrochemical deposition using a thin gold film (ca. 500 nm) on one side of the AAO template as working electrode with platinum wire (ϕ = 1 mm) as counter electrode and the saturated calomel electrode (SCE) as reference electrode.

SCHEME 1

4. Characterization of Templates and Nanowire Arrays. SEM (JEOL JSM 6700F) was employed to assess the structure of the templates as well as the nanowire arrays. To avoid charging effects while imaging, a thin layer of gold was sputtered onto the surface, and the images was acquired at electronvoltage (3.0 kV). The EDS was measured by EDAX phoenix. XPS was recorded using an ESCA LB200I-XL instrument (VG). XRD results were recorded using a Dmax 2000 spectrometer (Rigaku, CuKα). The conductive property of nanowires was investigated by C-AFM (Seiko, SPI 3800N) in the contact mode. A commercial Silicon cantilever (Type: SI-AF01-A) coated with gold was applied as scanning probe. The CITS mode was used during the acquisition of I−V curves. And the nominal spring constant of the cantilever estimates 0.1 N/m. The applied force was about 6 nN during the measurement. The samples were fixed on a metal plane with conductive gold paste to ensure ohmic electrical contact.

5. Experimental Method. The method for the synthesis of 1D materials using porous membranes as template was pioneered by Martin.[6] Electrodeposition is an attractive method for filling the high-aspect ratio pores of the template under ambient conditions, which provides exquisite control over the composition and growth rate.[7,8]

Figure 1 is a schematic illustration of the preparation of nanowire arrays of the dmit salt by electrochemical crystallization. An AAO template was made according to a reported procedure.[9] A gold film was evaporated onto one side of the AAO template and served as the working electrode for electrodeposition. The complex was deposited using a solution of 0.001 M $[(CH_3)_4N][Ni(dmit)_2]$ in acetonitrile containing $[(CH_3)_4N]$-

* Address correspondence to these authors. E-mail: wxu@iccas.ac.cn, jianglei@iccas.ac.cn.
† Chinese Academy of Sciences.
‡ Graduate School of Chinese Academy of Sciences.

10.1021/jp048195a CCC: $27.50
Published on Web 08/13/2004

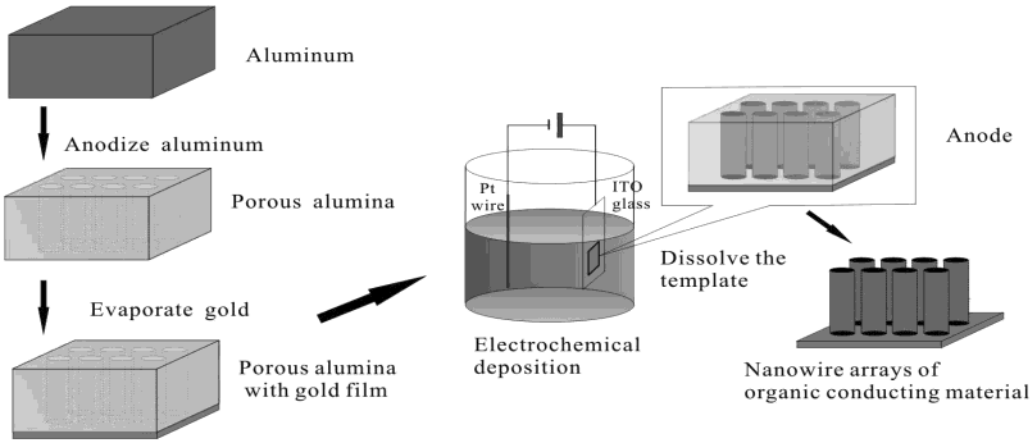

Figure 1. Schematic illustration of the fabricating nanowire arrays of crystalline $[(CH_3)_4N][Ni(dmit)_2]_2$ using AAO template.

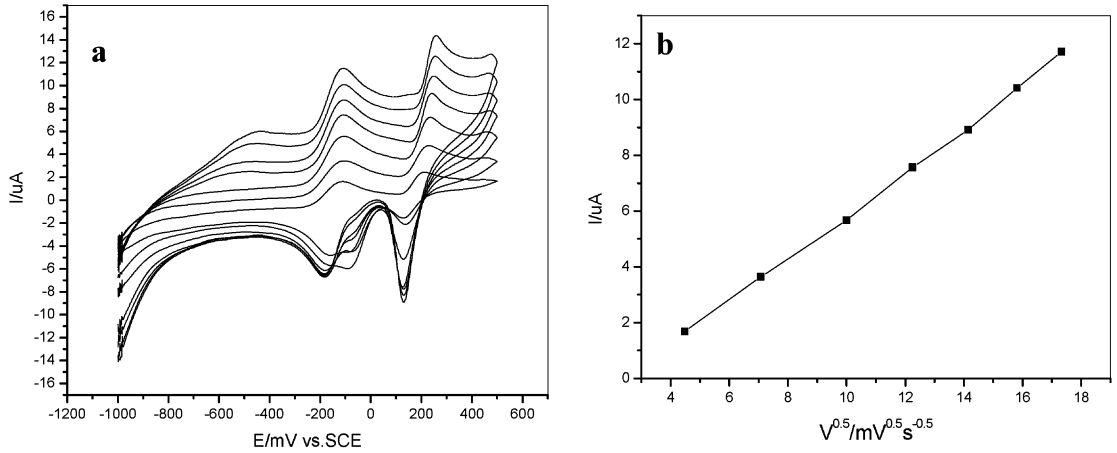

Figure 2. (a) Cyclic voltammograms of 0.001 M $[(CH_3)_4N][Ni(dmit)_2]$ in acetonitrile solution containing 0.1 M Bu_4NPF_6 as electrolyte at different scanning rates of 300 mV/s, 250 mV/s, 200 mV/s, 150 mV/s, 50 mV/s, and 20 mV/s in turn from outer to inner. (b) The linear relation between the current and the square root of the scanning rate at the first oxidation step.

$[ClO_4]$ as supporting electrolyte and Pt wire ($\phi = 1$ mm) as the counter electrode. $[Ni(dmit)]^-$ was oxidized to $[Ni(dmit)]^{\delta-}$ ($0 < \delta < -1$) and deposited on the surface of the anode. The electrodeposition was continued until the dmit salt grew to the top of the pores and overflowed the templates as determined by the color of the film changing to dark. Finally, the template was removed by soaking the samples in a NaOH solution (0.1 M) for several minutes. The template was then rinsed with water and dried under N_2 before being submitted to SEM investigation.

Results and Discussion

Cyclic voltammograms of $[(CH_3)_4N][Ni(dmit)_2]$ in acetonitrile were investigated (see Figure 2). The peak current was linear to the square root of the scanning rate at the first oxidation step at -106 mV from multiscanning voltammograms. This shows the electrochemical process was diffusion-controlled and adsorption phenomena were avoided. In the experiment, the growth of nanowires was processed under a conventional galvanostatic method and the first anodic peak was used as electrodeposition potential. Low current density (5∼10 μA cm^{-2}) was required to maintain the electrodeposition potential near -106 mV.

During the electrochemical deposition of the dmit salt nanowires, there was an evident oscillation of voltage which had a swing of about 2 mV with a period of about 25 s. The oscillation of voltage is shown in Figure 3. This oscillation may imply a corresponding influence on the structure of nanowires (it will be discussed in the following).

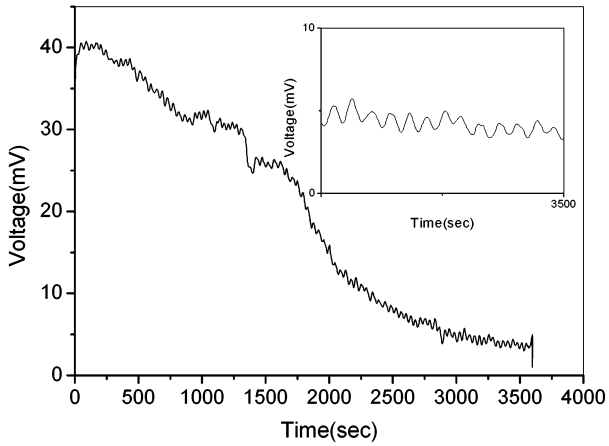

Figure 3. The voltage across the AAO/gold composite electrodes in a galvanostatic experiment (the current: 400 nA). The inset is a partially enlarged figure.

Figure 4a and 4b shows the SEM images of the dmit complex nanowires after the template has been partially dissolved; the top view of the nanowire arrays shows that more than 95% of the pores were filled with dmit complex (Figure 4a), which has caused these nanowires to be packed densely with each other. The tips of the nanowires are almost at the same level and the average diameter of the nanowires is 49 ± 2 nm, corresponding to the pore diameters of the AAO template. The side view of these nanowires shows that they stand on the substrate straight

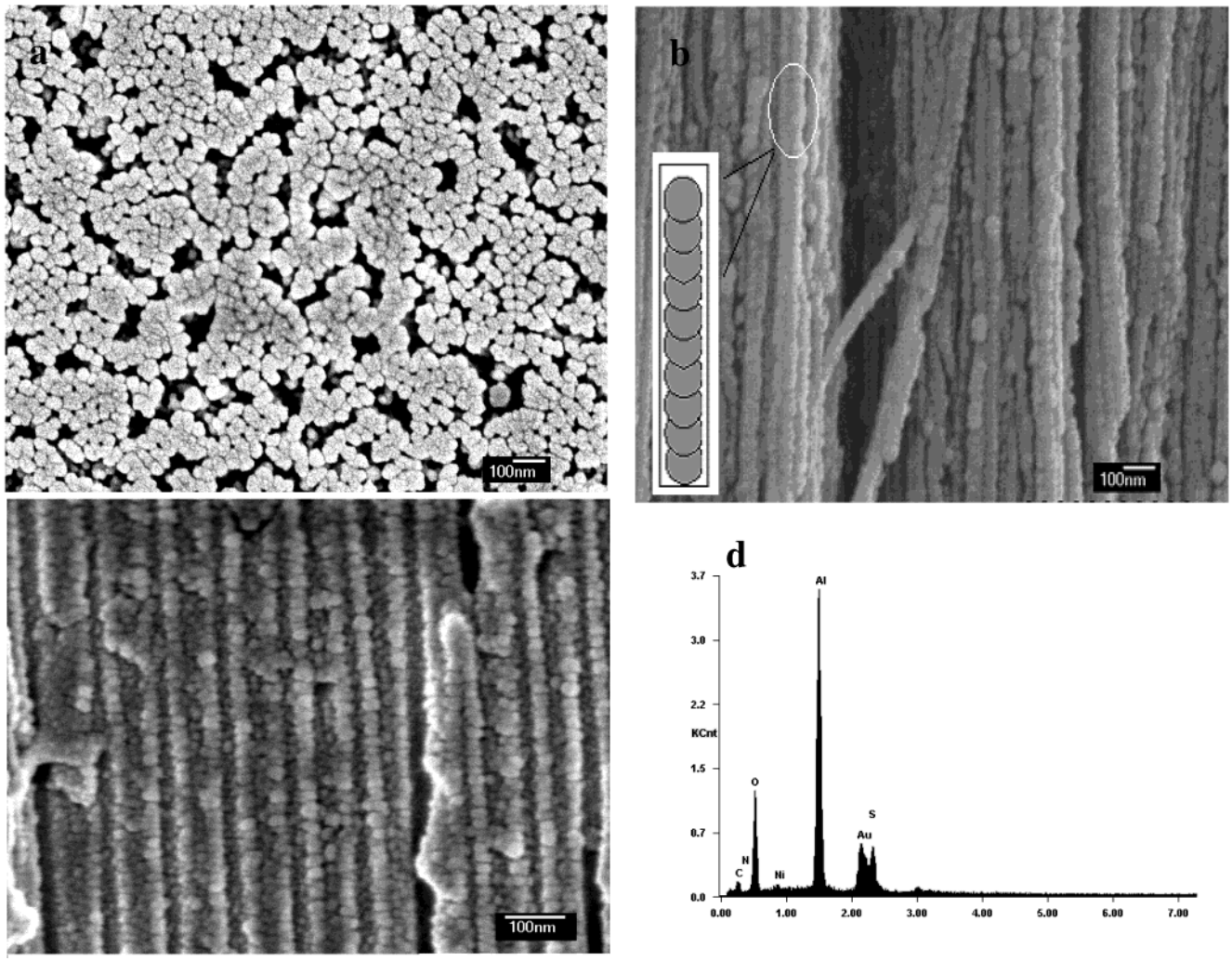

Figure 4. (a) SEM images of the top view of $[(CH_3)_4N][Ni(dmit)_2]_2$ nanowire arrays after the template was partially dissolved. The average pore diameter of template: 49 ± 2 nm. (b) SEM images of the side view of nanowire arrays in the template with the pore diameter of 49 ± 2 nm. (c) SEM images of the side view of nanowire arrays in the template with the pore diameter of 32 ± 4 nm. (d) EDS spectrum of the $[(CH_3)_4N][Ni(dmit)_2]_2$ nanowire arrays. It was measured from the cross section after partially dissolving the template for these images.

and separate from each other. The nanowires are about 30 μm long, corresponding to the thickness of the AAO template, and are continuous.

Detailed observation of the side view in Figure 4b clearly reveals that the nanowires possess periodic corrugated structures with a period of about 30 nm. Such structures make these wires look like straight pearl chains. Moreover, the smaller the diameter of the AAO is, the more evident the pearl chains are (see Figure 4c). Usually, the polymer nanostructures prepared by similar electrochemical deposition methods show smooth surfaces or surfaces with random roughness. A similar phenomenon, in which periodic nanostructures were associated with the oscillation of electric current or voltage, was first observed in the copper filaments during the electrochemical deposition on graphite in an ultrathin electrodeposition system by M. Wang et al.[10,11] In their papers, the composition analysis along the long axis of these copper filaments showed that the periodic structure was related to the fluctuation of Cu_2O concentration. That was explained by the fact that in the thin-layer electrodeposition system, ion transport is confined and the limited kinetic step is the transport of ion. The rapid consumption and slow compensation of Cu^{2+} at the surface of the working electrode resulted in the variation of concentration of Cu^{2+} and the equilibrium electrode potential of $Cu^{2+}|Cu$ during the electrodeposition and led to the deposition of the Cu_2O/Cu composite and Cu_2O alternately. In our case, the electrodeposition of the dmit salt was carried out in a confined one-

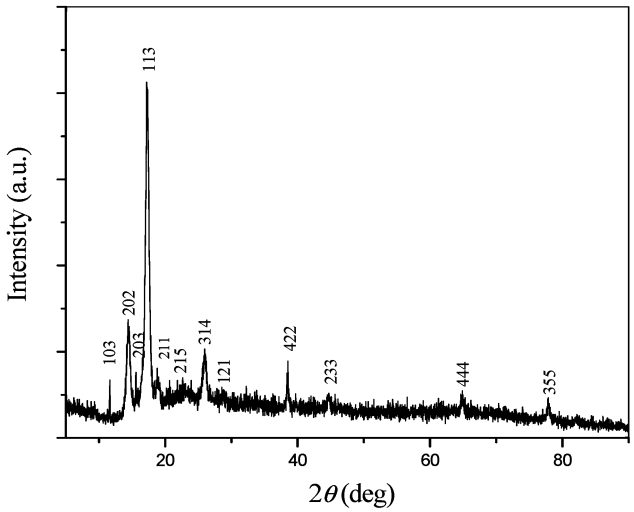

Figure 5. XRD pattern of $[(CH_3)_4N]$ $[Ni(dmit)_2]_2$ nanowire arrays on the top of the AAO template with the average pore diameter of 49 ± 2 nm. The position for $[(CH_3)_4N][Ni(dmit)_2]_2$ (103), (202), (113), (314), (422), (444), and (355) in the monoclinic crystal system are marked. The large (113) peak indicated a dominant $\langle 113 \rangle$ texture.

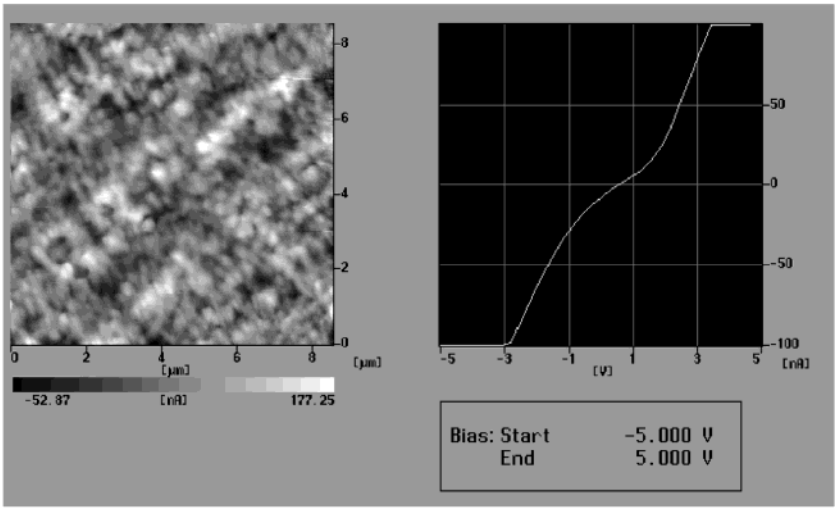

Figure 6. The C-AFM data of the $[(CH_3)_4N][Ni(dmit)_2]_2$ nanowire arrays. The left is a simultaneous current image of the nanowire arrays at a bias voltage of 5 V. After the template was partially dissolved, the C-AFM data was measured on the top of nanowire arrays with the average pore diameter of 49 ± 2 nm.

dimensional system. Similar to what happened in the above-mentioned two-dimensional system, the speed of the diffusion of the electric active species $[Ni(dmit)_2]^-$ was heavily suppressed. As the electrochemical deposition was a diffusion-controlled process, $[Ni(dmit)_2]^-$ was consumed rapidly, and the concentration of $[Ni(dmit)_2]^-$ decreased in front of the growing interface dramatically. The equilibrium electrode potential increased with the decreasing of the concentration of $[Ni(dmit)_2]^-$. At this time, the trace impurity of $[Ni(dmit)_2]^{2-}$ competed with the reaction. During the consumption of $[Ni(dmit)_2]^{2-}$, the concentration of $[Ni(dmit)_2]^-$ adjusted itself in front of the deposition interface and its electrodeposition was restarted. This procedure was repeated until the alumina pores were fully filled. The oscillation of voltage should also result from this procedure. On the periodic structures, one particle can correspond to one cycle of the above oscillation on the basis of our calculation. Because of the anisotropy of the growth of the crystal, this particle did not match the columned pore's shape completely but had a flat spherical shape. We can get evidence for the above supposition by comparing with the particle size and the period of the oscillation. It took us about 7 h to fill the template by electrodeposition under our experimental conditions. Considering the thickness of the template film was 30 μm and the period of voltage oscillation was about 25 s, the crystal growth in one period can be estimated as 30 nm long. This calculated value agrees well with that observed by SEM (length of spheres in the pearl chains are about 30 nm).

The composition and structure of these nanowires was further characterized with EDS, XPS, and XRD. Fixed-time EDS point analysis performed at random locations throughout the nanowire arrays after partial cleaving of the template and systematic line scans along the axis of a single nanowire both reveal that the composition is homogeneous. Traces of sulfate and nickel were detected. The binding energy of S2p (167.8 eV) was higher than those in the starting material. That is probably the result of the formation of partially oxidized species. The XRD peaks are all indexed to $[(CH_3)_4N][Ni(dmit)_2]_2$ in monoclinic crystal system based on cell parameters of $a = 13.654$ Å, $b = 6.426$ Å, $c = 35.709$ Å, and $\beta = 93.94°$. These cell parameters were obtained from the single crystal harvested from the standard bulk electrode under the identical electrochemical deposition conditions. It can be concluded that the nanowires were deposited in the AAO membrane containing the crystalline salt of $[(CH_3)_4N][Ni(dmit)_2]_2$. The intensity of the XRD peaks was so strong that the broad peak of the AAO template at ca. 23° was almost suppressed. The dominant (113) peak indicates that the wires were strongly textured with the (113) plane perpendicular to the wire axis. Organic conducting crystals are highly anisotropic materials and the crystals grow rapidly in the direction with higher conductivity.[3c] In the confined nanopores, the dmit complex crystals grow rapidly in the direction having the higher conductivity, which results in the highly oriented nanowire arrays.

The conductive properties of nanowires were characterized by conductive atomic force microscopy (C-AFM). The bright area in the current image implies a high conductivity. The right is a representative I−V curve. When the figure of voltage exceeded 3 V, the current went beyond the limit and presented a straight line in the I−V curve. The preliminary results show that the conductivities of these nanowires are variable in a range from 10 to 0.1 $S \cdot cm^{-1}$. (This result was based on the supposition that the current at a particular point flew through a single nanowire.) This value is much higher than that measured using a two-electrode method ($\sim 5 \times 10^{-3}$ $S \cdot cm^{-1}$) by more slowly evaporating another gold film electrode on the opposite side of the as-prepared sample. However, it is much lower than that reported by Kobayashi et al. measured on a bulk single crystal.[12] This may be because the pearl chainlike nanowires are not single crystals.

Conclusion

Nanowire arrays of crystalline $[(CH_3)_4N][Ni(dmit)_2]_2$ with a nanosized diameter have been fabricated. A nanopearl chain associated with the oscillation of the voltage during the electrochemical deposition was observed. These nanowire arrays were highly textured in the direction with higher conductivity. For organic molecular conducting materials, it is important to form a highly oriented low dimensional crystal for practical application.

Acknowledgment. This work was supported by the Chinese Academy of Sciences, NSFC, and the State Basic Research Development Program.

Supporting Information Available: Large scale SEM image of the side view of the nanowire arrays. This material is available free of charge via the Internet at http://pubs.acs.org.

References and Notes

(1) See, for example, (a) Ozin, G. A. *Adv. Mater.* **1992**, *4*, 612. (b) Duan, X.; Huang, Y.; Cui, Y.; Wang, J.; Lieber, C. M. *Nature* **2001**, *409*, 66. (c) Baughman, R. H.; Zakhidov, A. A.; de Heer, W. A. *Science* **2002**, *297*, 787.

(2) See, for example, (a) Burford, R. P.; Tongtam, T. *J. Mater. Sci.* **1991**, *26*, 3264. (b) Tans, S. J.; Verschueren, A. R. M.; Dekker, C. *Nature* **1998**, *393*, 49. (c) Cai, Z.; Martin, C. R. *J. Am. Chem. Soc.* **1989**, *111*, 4138.

(3) (a) Liu, H.; Li, Y.; Jiang, H.; Luo, H.; Xiao, S.; Fang, H.; Li, H.; Zhu, D.; Yu, D.; Xu, J.; Xiang, B. *J. Am. Chem. Soc.* **2002**, *124*, 13370. (b) Kim, Y.; Mayer, M. F.; Zimmerman, S. C. *Angew. Chem., Int. Ed.* **2003**, *42*, 1121. (c) Favier, F.; Liu, H.; Penner, R. M. *Adv. Mater.* **2001**, *13*, 1567.

(4) (a) Williams, J. M.; Ferraro, J. R.; Thorn, R. J.; Carlson, K. D.; Geiser, U.; Wang, H.; Kini, A. M.; Whangbo, M. H. *Organic Superconductors (Including Fullerenes): Synthesis, Structure, Properties and Theory*; Prentic Hall: Englewood Cliffs, New Jersey, 1992. (b) Tanaka, H.; Okano, Y.; Kobayashi, H.; Suzuki, W.; Kobayashi, A. *Science* **2001**, *291*, 285. (c) Itkis, M. E.; Chi, X.; Cordes, A. W.; Haddon, R. C. *Science* **2002**, *296*, 1443.

(5) (a) Mukai, K.; Senba, N.; Hatanaka, T.; Minakuchi, H.; Ohara, K.; Taniguchi, M.; Misaki, Y.; Hosokoshi, Y.; Inoue, K.; Azuma, N. *Inorg. Chem.* **2004**, *43*, 566. (b) Akutagawa, T.; Hashimoto, A.; Nishihara, S.; Hasegawa, T.; Nakamura, T. *J. Phys. Chem. B* **2003**, *107*, 66. (c) Kobayashi, A.; Suzuki, W. *Mol. Cryst. Liq. Cryst.* **2002**, *380*, 37. (d) Akutagawa, T.; Hasegawa, T.; Nakamura, T.; Inabe, T. *J. Am. Chem. Soc.* **2002**, *124*, 8903. (e) Caro, D. de; Fraxedas, J.; Faulmann, C.; Malfant, I.; Milon, J.; Lamère, J.-F.; Collière, V.; Valade, L. *Adv. Mater.* **2004**, *16*, 835.

(6) Sun, S.; Wu, D.; Zhu, D. *Chin. Chem. Lett.* **1996**, *7*, 1054.

(7) Martin, C. R. *Science* **1994**, *266*, 1961. (b) Helteen, J. C.; Martin, C. R. *J. Mater. Chem.* **1997**, *7*, 1075. (c) Martin, C. R. *Acc. Chem. Res.* **1995**, *28*, 61.

(8) Prieto, A. L.; Martin-González, M.; Keyani, J.; Gronsky, R.; Sands, T.; Stacy, A. M. *J. Am. Chem. Soc.* **2003**, *125*, 2388. (b) Choi, J.; Saucer, G.; Nielsch, K.; Wehrspohn, R. B.; Gösele, U. *Chem. Mater.* **2003**, *15*, 776.

(9) Prieto, A. L.; Sander, M. S.; Martin, M. S.; Gonzalez, M.; Gronsky, R.; Sands T.; Stacy, A. M. *J. Am. Chem. Soc.* **2001**, *123*, 7160.

(10) Wang, M.; Zhong, S.; Yin, X. B.; Zhu, J. M.; Peng, R. W.; Wang, Y.; Zhang, K.; Ming, N. B. *Phys. Rev. Lett.* **2001**, *86*, 3827.

(11) Zhong, S.; Wang, Y.; Wang, M.; Zhang, M. Z.; Yin, X. B.; Peng, R. W.; Ming, N. B. *Phys. Rev. E* **2003**, *67*, 061601−1.

(12) Kim, H.; Kobayashi, A.; Sasaki, Y.; Rato, R.; Kobayashi, H. *Chem. Lett.* **1987**, 1799.